3D graphene network investigation by Raman spectroscopy

C. BANCIU*, M. LUNGULESCU, A. BĂRA, L. LEONAT, A. TEIȘANU
National Institute for Research and Development in Electrical Engineering INCDIE ICPE-CA, 313 Splaiul Unirii, 030138, Bucharest 3, Romania

Graphene is a carbon material with an outstanding combination of beneficial properties, of interest for various practical applications in electronic, optoelectronic, and energy storage devices. In this paper, we prepare a 3D graphene network by using nickel foam as template in a chemical vapour deposition (CVD) process with methane as the carbon source. The obtained graphene network on nickel foam does not present notable defects as shown from scanning electron microscopy and Raman spectroscopy. Raman spectroscopy is used to evaluate the influence of the deposition time on the thickness of graphene layers as well as to evaluate their structural properties.

(Received December 6, 2016; accepted June 7, 2017)

Keywords: 3D graphene, Nickel foam, Raman spectroscopy, Optoelectronics

1. Introduction

Graphene is a distinctive two-dimensional carbon material, in fact a monolayer of carbon atoms arranged into a honeycomb type structure, which was recognized for its special physical, chemical, optical and electrical properties [1-4]. Graphene has been widely used as an electrode material in detection and power devices, with higher electrochemical performance in comparison to noble metals and to electrode materials based on carbon, such as graphite and carbon nanotubes [2, 3, 6]. Graphene is also used in various applications such as rechargeable lithium batteries [7], supercapacitors [8], fuel cell devices [9, 10], in sensing [2, 11-14], and terahertz applications [15, 16].

Graphene has high mobility and optical transparency, in addition to flexibility, robustness and environmental stability. Thus, graphene has a true potential in photonics and optoelectronics, where the combination of its unique optical and electronic properties can be fully exploited [17].

For the outstanding electrical, optical, and mechanical properties, graphene has emerged as vital components of dye-sensitized solar cells (DSSCs) [18–20]. As a photoanode in dye-sensitized solar cells, graphene was first used in 2008 as a transparent electrode to replace FTO [21]. By adding graphene to conducting polymers, the electrocatalytic activity of the counter electrodes in DSSC can be enhanced owing to large surface area, high electrical conductivity and high charge carrier mobility offered by graphene [22, 23].

Gao et al. adopted graphene-TiO_2 (0.5% wt. graphene) to fabricate the photoanode for DSSCs, and the obtained power conversion efficiency (η) is much higher than that of the pure TiO_2 photoanode based sample [24]. Chen et al. reported graphene assisted P25 photoanode and obtained a 15% increase for the η [25]. Other researchers prepared DSSCs with a graphene modified photoanode, and the η as high as ~9% [26, 27].

The use of graphene involves some experimental problems which could be overcome by using 3D graphene foam, which has a porous macrostructure with the microscopic characteristics of graphene [28]. Such three-dimensional structures of graphene give a large active specific surface area, which in combination with the unique properties of graphene have the potential to be useful in the field of electrochemistry, electronics and optoelectronics.

The concept of the 3D macro structure of graphene was originally conceived by Chen et al. [29, 30], when they grew graphene by chemical vapour deposition (CVD) on a 3D skeleton of nickel [31].

Due to the fact that the structure of the 3D graphene is monolithic in comparison to the reduced graphene oxide obtained by electrochemical route or with the graphene nanoflakes with several layers, which are formed from distinct thin graphene sheets connected to each other, the electrical and structural properties of the graphene foam will be excellent in comparison to the properties of two-dimensional graphene that have a large number of defects and poor mechanical contact between the flakes. In addition, the reduced graphene oxide is inherently less conductive than the graphene which the 3D structure is made up of.

In general, a characterization technique must meet several conditions: to be quick and non-destructive, providing high resolution, and to give structural and electronic information. Raman spectroscopy meets all these requirements and has become one of the most popular methods for characterizing amorphous carbon materials and with a certain degree of structural disorder.

In particular, Raman spectroscopy is used for graphene [32] because the absence of the band gap makes all incidents wavelengths to be resonant, so Raman spectra contain information about the atomic structure and the electronic properties. Raman spectra are characterized by

the presence of two major bands known as a "G band" and "2D band". If graphene presents structural defects, then the Raman spectrum will contain a third band, "D band".

The CVD method was shown to produce high-quality graphene [33] that display fewer structural defects in comparison to the reduced graphene oxide (rGO) sheets produced by the chemical route.

In this paper, we prepare the graphene network by using Ni foam as the template in a CVD process with methane as carbon source. The obtained graphene network on Ni foam was investigated by Raman spectroscopy in order to evaluate the influence of deposition time on the thickness of graphene layer.

2. Experimental

A commercial nickel foam produced by Gelon LIB Group (number of pores per inch: 110 PPI, density ≥ 250 g/m^2, thickness ≤ 2.5 mm) served as template. Graphene networks were obtained by synthesis on the Ni foam through a CVD process with methane (CH_4) as carbon source at 1273.15 K under ambient pressure. Graphene sheets copied the structure of the nickel foam resulting in a network with identical structure as the Ni foam template. Different deposition times were used in order to determine the influence of deposition time on the thickness of the deposited graphene layer.

The nickel foam, previously cleaned with acetone and isopropyl alcohol by sonication, was loaded into a CVD furnace (model EasyTube 2000 produced by CVD Equipment Corporation USA) and heated up to 1273.15 K. The sample was annealed at 1273.15 K for 15 minutes under an atmosphere of argon (Ar) and hydrogen (H_2). The graphene growth was then carried out at 1273.15 K for 5, 15 and 30 minutes under a gas mixture of $1.67 \cdot 10^{-5}$ m^3/s Ar, $3.33 \cdot 10^{-6}$ m^3/s CH_4 and $5.42 \cdot 10^{-6}$ m^3/s H_2 at atmospheric pressure. Finally, the sample was rapidly cooled to room temperature under the protection of Ar and H_2.

The CVD process conditions for graphene networks (GN) preparation are presented in the Table 1.

Table 1. CVD process conditions for graphene networks preparation

Sample	Growing time (minutes)	Growing temperature (K)	CH_4 flow rate (m^3/s)	H_2 flow rate (m^3/s)
GN_CVD_5	5	1273.15	$3.33 \cdot 10^{-6}$	$5.42 \cdot 10^{-6}$
GN_CVD_15	15			
GN_CVD_30	30			

The morphology of nickel foam and graphene layers deposited on nickel foam was observed using an Auriga Station Scanning Electron Microscope from Carl Zeiss at different magnifications.

The obtained 3D graphene network on Ni foam was investigated by Raman spectroscopy in order to identify structural defects. The Raman spectroscopy was also very useful to determine the number of layers in the graphene networks, which is directly influenced by the growing time.

Raman spectroscopy was performed using a dispersive Raman Spectrometer model LabRAM HR Evolution Horiba.

In order to avoid the sample from heating, we used an excitation laser with the wavelength of 532 nm and the power of 5 mW. The Raman spectra were acquired in the spectral range of 100-3400 cm^{-1} at an acquisition time of 10 seconds with 10 accumulations using a diffraction grating with 600 grooves/mm and 50x objective lens with numerical aperture of 0.75.

3. Results and discussion

Fig. 1 displays the raw nickel foam structure at different magnifications (100 X, 1000 X).

Figs. 2, 3 and 4 show the graphene networks resulted after the CVD synthesis on the Ni foam for 5, 15 and 30 minutes at different magnifications (1000 X, 5000 X).

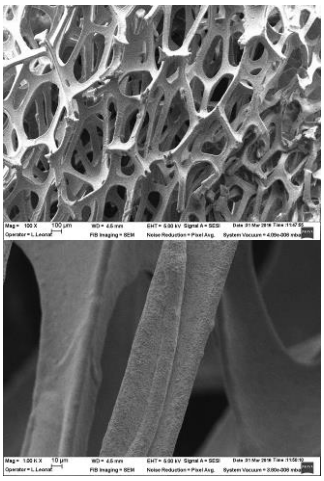

Fig. 1. SEM images of a commercial nickel foam

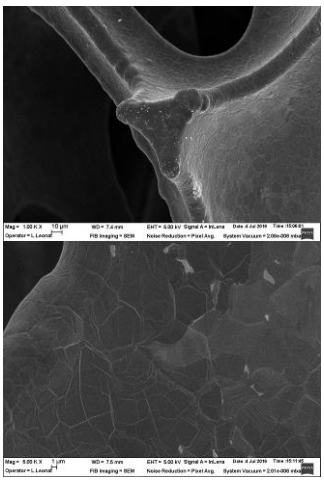

Fig. 2. SEM images of graphene network obtained by CVD process at growing time 5 minutes

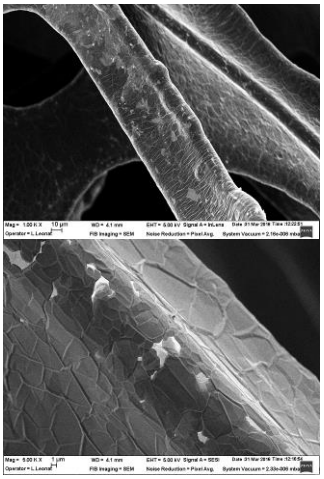

Fig. 3. SEM images of graphene network obtained by CVD process at growing time 15 minutes

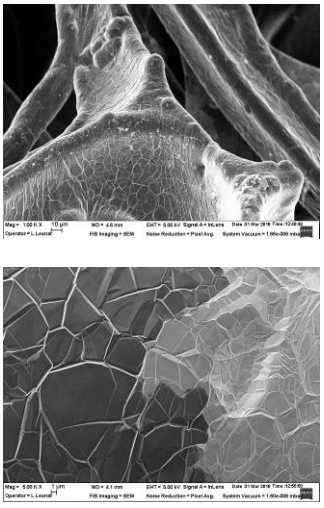

Fig. 4. SEM images of graphene network obtained by CVD process at growing time 30 minutes

At higher magnification the specific structure of graphene can be observed. A closer look on the high magnification SEM images reveals that the graphene layers fully cover the nickel foam, even at a growing time of 5 minutes. These findings are in good agreement with previously achieved results from the scientific literature [29]. Even at the highest synthesis interval of 30 minutes, graphene coverage is smooth and continuous and there are not defects such as graphite microspheres which are known to form when prolonged synthesis is applied [34].

Fig. 5 presents the Raman spectra of CVD graphene networks grown on Ni foam for 5 minutes.

Fig. 6 presents the Raman spectra of CVD graphene networks obtained at different growing times.

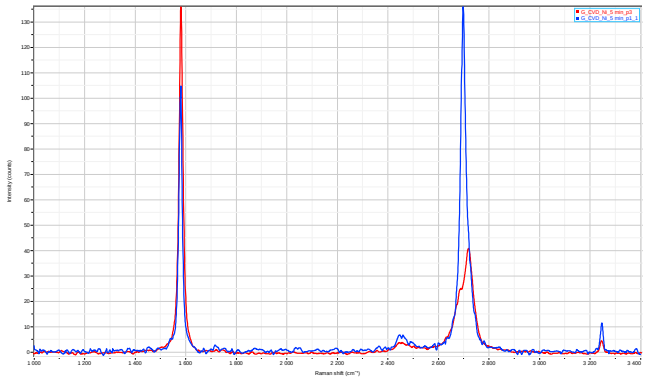

Fig. 5. Raman spectra of graphene network obtained by CVD process at a growing time of 5 minutes in 2 spots

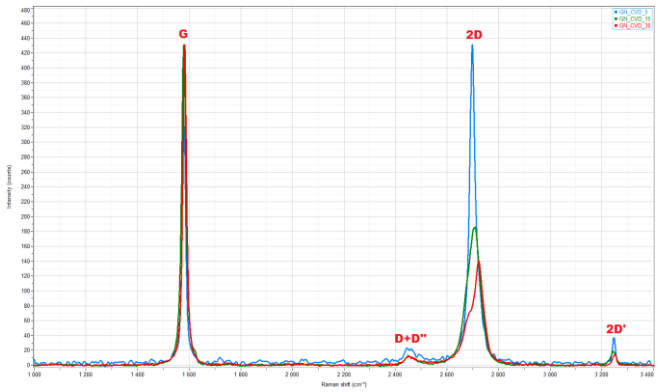

Fig. 6. Raman spectra of graphene networks obtained by CVD process at growing times of 5, 15 and 30 minutes

Table 2 presents the values of the Raman peaks of G and 2D band obtained for graphene networks, the ratio of the peak intensities I_{2D}/I_G and the full width at half-maximum (FWHM) of the G and 2D band.

Table 2. Raman shifts of G and 2D band obtained for graphene networks

Growing time (minutes)	G band (cm^{-1})	2D band (cm^{-1})	I_{2D}/I_G	FWHM G band (cm^{-1})	FWHM 2D band (cm^{-1})
5	1579	2698	1.24	15	27
15	1580	2708	0.43	18	50
30	1582	2718	0.31	17	56

From the Raman spectra we can observe in Fig. 5 that the graphene grown by CVD on Ni foam in 5 minutes presents a different number of layers in two different spots. For a spot the Raman spectrum suggests a bi-layer structure (blue line) and for another spot a multi-layer structure (red line). The ratio I_{2D}/I_G of a single-layer graphene is equal or more than 2, for bi-layer graphene between 1 and 2 and for

multi-layer graphene less than 1, according to data from scientific literature [35].

In Fig. 6 we can observe that the G and 2D peaks position is almost the same like in graphite (G band at around 1580 cm^{-1} and 2D band at around 2700 cm^{-1}). The intensity of G peak increases with the number of layers, in the same time with the decreasing of the intensity of 2D peak. In our case, the ratio of the intensities I_{2D}/I_G decreases from 1.24 to 0.31. This indicates an increase in the number of graphene layers.

The absence of the D band, which characterizes the disorder degree of sp^2 materials [36], may indicate either low defect content [32, 37] or the D peak is invisible because of crystal symmetries (pristine graphene) [38].

It must be noted that there is a variation of the Raman G peak position and width, which may be attributed to electronic doping by substrate [39, 40], or to the presence of charges and a compressive strain in the graphene samples [37, 41].

The full width of the 2D band at half maximum ($FWHM_{2D}$) is a quantitative guide to distinguish the number of layers. As for single-layer graphene, the 2D band is symmetric and can be fitted into only one Lorentzian peak [42]. Here, $FWHM_{2D}$ of the sample GN_CVD_5 is 27 cm^{-1}, a value corresponding to a single-layer graphene. The Raman spectrum of multi-layer graphene GN_CVD_15 has a wider $FWHM_{2D}$ of 50 cm^{-1}, more than twice than that of GN_CVD_5. The $FWHM_{2D}$ of the GN_CVD_30 is slightly bigger than that of GN_CVD_15 (56 cm^{-1}).

The position of the Raman 2D peak for multilayer graphene is, also blue-shifted with about 10 cm^{-1}, relative to monolayer graphene, indicating a misoriented multilayer graphene [43-45]. The increase of the 2D peak width was observed by Pimenta et al. [46] in turbostratic multilayer graphite. Based on these evidences we can conclude that our obtained CVD graphene are misoriented or turbostratic multilayer graphene.

4. Conclusions

The 3D graphene structures were obtained by CVD synthesis with methane as carbon source using different deposition times: 5, 15 and 30 minutes.

The samples were characterized by scanning electron microscopy, Raman spectroscopy and neutron scattering investigations.

Raman spectroscopy has become ubiquitous for characterizing all type of carbon materials. The positions, widths and intensities of the D, G and 2D peaks made it possible to determine the number of layers and the disorder in a graphene structure. Thus, Raman spectroscopy is a powerful and noninvasive tool for graphene characterization. According to the Raman spectra, we can conclude that the number of layers increases with the growing time. However, at all growing times, the graphene layers were smooth, continuous and no defects were observed. The absence of D band proves a low defect content.

Acknowledgments

The work has been funded by the financial support of the UEFISCDI, project no. 129PED/2017, the Bilateral Collaboration Romania-Russia, project position 37 from the JINR Order no. 96/15.02.2016, and the CORE Research Programme, project no. PN 1611-0202/2016.

References

[1] K. S. Novoselov, A. K. Geim, S. V. Morozov, D. Jiang, et al., Science **306**(5696), 666 (2004).
[2] D. A. C. Brownson, C. E. Banks, Analyst **135**(11), 2768 (2010).
[3] M. Pumera, Chem. Rec. **9**(4), 211 (2009).
[4] A. K. Geim, K. S. Novoselov, Nat. Mater. **6**, 183 (2007).
[5] D. A. C. Brownson, L. J. Munro, D. K. Kampouris, C. E. Banks, RSC Advances **1**, 978 (2011).
[6] D. A. C. Brownson, D. K. Kampouris, C. E. Banks, J. Power Sources **196**, 4873 (2011).
[7] S. M. Paek, E. Yoo, I. Honma, Nano Lett. **9**, 72 (2009).
[8] H. Wang, Q. Hao, X. Yang, L. Lu, X. Wang, Electrochem. Commun. **11**, 1158 (2009).
[9] C. Liu, S. Alwarappan, Z. Chen, X. Kong, C. Z. Li, Biosens. Bioelectron. **25**, 1829 (2010).
[10] R. I. Jafri, N. Rajalakshmi, S. Ramaprabhu, J. Mater. Chem. **20**, 7114 (2010).
[11] X. Kang, J. Wang, H. Wu, J. Liu, I. A. Aksay, Y. Lin, Talanta **81**, 754 (2010).
[12] Y. R. Kim, S. Bong, Y. J. Kang, Y. Yang, R. K. Mahajan, J. S. Kim, H. Kim, Biosens. Bioelectron. **25**, 2366 (2010).
[13] X. Kang, J. Wang, H. Wu, I. A. Aksay, J. Liu, Y. Lin, Biosens. Bioelectron. **25**, 901 (2009).
[14] Y. Wang, Y. Wan, D. Zhang, Electrochem. Commun. **12**, 187 (2010).
[15] S. Yamacli, J. Optoelectron. Adv. M. **18**(9-10), 803 (2016).
[16] L. Li, M Cao, L. Meng, J. Optoelectron. Adv. M. **17**(11-12), 1650 (2015).
[17] F. Bonaccorso, Z. Sun, T. Hasan, A. C. Ferrari, Nature Photonics **4**, 611 (2010).
[18] Y. Zhang, H. Li, L. Kuo, P. Dong, F. Yan, Curr. Opin. Colloid Interface Sci. **20**, 406 (2015).
[19] M. Ye, X. Wen, M. Wang, J. Iocozzia, N. Zhang, C. Lin, Z. Lin, Mater. Today **18**, 155 (2015).
[20] Y. Yang, S. Li, L. Zhang, J. Xu, W. Yang, Y. Jiang, ACS Appl. Mater. Interfaces **5**, 4350 (2013).
[21] X. Wang, L. Zhi, K. Müllen, Nano Lett. **8**, 323 (2008).
[22] G. Yue, J. Wu, Y. Xiao, J. Lin, M. Huang, Z. Lan, L. Fan, Energy **54**, 315 (2013).
[23] M. S. Rahman, W. A. Hammed, R. B. Yahya, H. N. M. Ekramul Mahmud, J. Polym. Res. **23**, 192 (2016).
[24] P. Dong, C. L. Pint, M. Hainey, F. Mirri, et al., ACS Appl. Mater. Interf. **3**, 3157 (2011).
[25] T. H. Tsai, S. C. Chiou, S. M. Chen, Int. J. Electrochem. Sci. **6**, 3333 (2011).
[26] B. Tang, G. X. Hu, J. Power Sources **220**, 95 (2012).

[27] B. Tang, G. Hu, H. Gao, Z. Shi, Journal of Power Sources **234**, 60 (2013).
[28] D. A. C. Brownson, L. C. S. Figueiredo-Filho, X. Ji, et al., J. Mater. Chem. A **1**, 5962 (2013).
[29] Z. Chen, W. Ren, L. Gao, B. Liu, S. Pei, H.-M. Cheng, Nat. Mater. **10**, 424 (2011).
[30] Z. Chen, C. Xu, C. Ma, W. Ren, H. M. Cheng, Adv. Mater. **25**(9), 1296 (2013).
[31] L. C. S. Figueiredo-Filho, D. A. C. Brownson, O. Fatibello-Filho, C. E. Banks, Electroanalysis **26**(1), 93 (2014).
[32] A. C. Ferrari, Solid State Comm. **143**(1-2), 47 (2007).
[33] X. S. Li, W. W Cai, J. H. An, S. Kim, et al., Science **324**, 1312 (2009).
[34] W. Li, S. Gao, L. Wu, S. Qiu, et al., Sci. Rep. **3**, 2125 (2013).
[35] V. T. Nguyen, H. D. Le, V. C. Nguyen, et al., Adv. Nat. Sci.: Nanosci. Nanotechnol. **4**, 035012 (2013).
[36] M. S. Dresselhaus, A. Jorio, A. G. Souza Filho, R. Saito, Phil. Trans. R. Soc. A **368**, 5355 (2010).
[37] L. M. Malard, M. A. Pimenta, G. Dresselhaus, M. S. Dresselhaus, Phys. Rep. **473**, 51 (2009).
[38] F. Tuinstra, L. Koenig, J. Chem. Phys. **53**, 1126 (1970).
[39] A. C. Ferrari, J. C. Meyer, V. Scardaci, C. Casiraghi, et al., Phys. Rev. Lett. **97**, 187401-4 (2006).
[40] C. Casiraghi, S. Pisana, K. S. Novoselov, et al., Appl. Phys. Lett. **91**, 233108 (2007).
[41] J. Rohr, M. Hundhausen, K. V. Emtsev, et al., Appl. Phys. Lett. **92**, 201918 (2008).
[42] Y. Hao, Y. Wang, L. Wang, et al., Small **6**(2), 195 (2010).
[43] P. Poncharal, A. Ayari, T. Michel, J. Sauvajol, Phys. Rev. B **78**, 113407 (2008).
[44] D. R. Lenski, M. S. Fuhrer, J. Appl. Phys. **110**, 013720 (2011).
[45] C. Faugeras, A. Nerrière, M. Potemski, A. Mahmood, et al., Appl. Phys. Lett. **92**, 011914 (2008).
[46] M. A. Pimenta, G. Dresselhaus, M. S. Dresselhaus, L. G. Cancado, Phys. Chem. Chem. Phys. **9**, 1276 (2007).

*Corresponding author: cristina.banciu@icpe-ca.ro